Bioorganic & Medicinal Chemistry Letters 27 (2017) 2153–2160

Contents lists available at ScienceDirect

Bioorganic & Medicinal Chemistry Letters

journal homepage: www.elsevier.com/locate/bmcl

Design, synthesis and optimization of bis-amide derivatives as CSF1R inhibitors

Sreekanth A. Ramachandran [a], Pradeep S. Jadhavar [a], Sandeep K. Miglani [a], Manvendra P. Singh [a], Deepak P. Kalane [a], Anil K. Agarwal [a], Balaji D. Sathe [a], Kakoli Mukherjee [a], Ashu Gupta [a], Srijan Haldar [a], Mohd Raja [a], Siddhartha Singh [a], Son M. Pham [b], Sarvajit Chakravarty [b], Kevin Quinn [b], Sebastian Belmar [c], Ivan E. Alfaro [c], Christopher Higgs [d], Sebastian Bernales [b], Francisco J. Herrera [b], Roopa Rai [b,*]

[a] Integral BioSciences Pvt. Ltd, C-64, Hosiery Complex Phase II Extension, Noida, Uttar Pradesh 201306, India
[b] Medivation, now Pfizer, 525 Market Street, 36th Floor, San Francisco, CA 94105, USA
[c] Fundación Ciencia y Vida, Avenida Zañartu 1482, Ñuñoa, Santiago 778027, Chile
[d] Schrödinger, Inc., 120 West 45th Street, 17th Floor, New York, NY 10036, USA

ARTICLE INFO

Article history:
Received 31 December 2016
Revised 18 March 2017
Accepted 22 March 2017
Available online 24 March 2017

Keywords:
CSF1R
FMS
Inhibitors
Bis-amides

ABSTRACT

Signaling via the receptor tyrosine kinase CSF1R is thought to play an important role in recruitment and differentiation of tumor-associated macrophages (TAMs). TAMs play pro-tumorigenic roles, including the suppression of anti-tumor immune response, promotion of angiogenesis and tumor cell metastasis. Because of the role of this signaling pathway in the tumor microenvironment, several small molecule CSF1R kinase inhibitors are undergoing clinical evaluation for cancer therapy, either as a single agent or in combination with other cancer therapies, including immune checkpoint inhibitors. Herein we describe our lead optimization effort that resulted in the identification of a potent, cellular active and orally bioavailable bis-amide CSF1R inhibitor. Docking and biochemical analysis allowed the removal of a metabolically labile and poorly permeable methyl piperazine group from an early lead compound. Optimization led to improved metabolic stability and Caco2 permeability, which in turn resulted in good oral bioavailability in mice.

CSF1R (also referred to as FMS) is the receptor for the colony stimulating factor (CSF1) which regulates the survival and differentiation of macrophages.[1,2] This receptor tyrosine kinase is expressed in several tumor types where it regulates tumor associated macrophages (TAMs). TAMs play pro-tumorigenic roles in the tumor microenvironment (TME) by stimulating angiogenesis, promoting tumor cell invasion and inducing an immunosuppressive environment.[2–4] Given the key roles which TAMs plays in modulating the TME, altering their activity by blocking CSF1R signaling has been indicated as a possible anti-cancer strategy, particularly in combination with immune checkpoint therapies.[4–6]

A survey of the literature revealed five orally active small molecule CSF1R inhibitors currently under clinical development. These are shown in Fig. 1. PLX3397, an inhibitor of CSF1R and c-Kit, is the most advanced compound, currently undergoing Phase 3 clinical studies in patients with tenosynovial giant cell tumor (TGCT).[7] BLZ945 is a selective CSF1R kinase inhibitor currently undergoing Phase 1/2 study either as a single agent or in combination with anti-PD-1 antibody in advanced solid tumors.[5] PLX7486 (structure not disclosed), a CSF1R and Trk inhibitor, has also advanced to Phase 1 trial in patients with advanced solid tumors.[8] ARRY-382 (structure not disclosed), is undergoing Phase 1/2 dose escalation trial in combination with the anti-PD-1 antibody pembrolizumab (Keytruda®), in patients with advanced solid tumors.[9] JNJ-40346527, a selective inhibitor of CSF1R was well tolerated, and preliminary antitumor results from Phase 1/2 suggested limited activity in monotherapy for the treatment of relapsed or refractory classical Hodgkin lymphoma (cHL).[10] Antibodies against CSF1 and CSF1R have also been developed, some of which are undergoing clinical trials.[4]

Our search began with bis-amide **1** (Table 1), a compound reported in the literature to be a mixed kinase inhibitor with activity against both c-Kit and CSF1R. c-Kit is a closely related homolog of CSF1R and plays key roles in several physiological processes including the regulation of hematopoietic stem cells.[11] To avoid potential effects of c-Kit inhibition on hematopoiesis, we targeted compounds that would preferentially inhibit CSF1R over c-Kit.

* Corresponding author.
E-mail address: roopa.rai@hotmail.com (R. Rai).

http://dx.doi.org/10.1016/j.bmcl.2017.03.064
0960-894X/

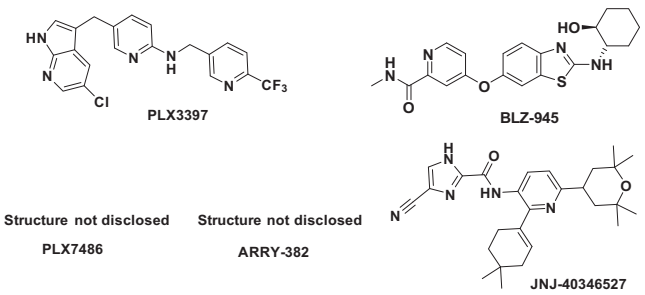

Fig. 1. Reported CSF1R inhibitors in clinical development.

Thus, our screening cascade involved the biochemical potency measurement of newly synthesized compounds against CSF1R and c-Kit. The enzymatic activity was determined in vitro using the indicated enzymes incubated with [ϒ-^{33}P]-ATP and peptide substrate. IC_{50} curves were determined for each compound (see Supplemental information). These biochemical assays were followed by testing our compounds in cell viability assays using mouse bone marrow-derived macrophages (BMM), a primary cell culture known to require CSF1 for viability.[12] Viability assays using the RAW 264.7 cell line were included as an indication for general off-target activity since this cell line does not require CSF1 for its viability.

With the aim of identifying a CSF1R inhibitor with improved selectivity over c-Kit, our search began with the synthesis of analogs of the bis-amide **1**.[13] With the corresponding phenyl core replacing the pyridine (**2**), we made a series of compounds shown in Table 1. In order to understand the importance of the trifluoromethyl group at R^3, we synthesized compound **3** (R^3 = H) which was inactive towards CSF1R kinase when tested up to 10 μM concentration. Compound **4**, where a chlorine replaces the trifluoromethyl group resulted in moderate potency towards CSF1R. Similarly, the role of R^2 methyl group was explored by replacing it with chlorine (compound **5**) wherein the CSF1R potency was retained, indicating that the potency was not impacted by varying the electronics of the phenyl ring. The original 2-thiophene substituent at R^1, off the phenyl group, was replaced with a pyridine (compound **6**) and pyrimidine (compound **7**); this resulted in a 4–8-fold CSF1R potency improvement. This biochemical potency improvement also translated to ~60% inhibition of BMM cell viability when tested at 1 μM. All these compounds were not cytotoxic when tested in RAW 264.7 cells at 1 μM.

Next, single-point changes to the amide linkers were made to understand the role of the 2 amide bonds in the compounds described in Table 1. Amide bonds may provide specific hydrogen-bonding interactions with the target protein and play a role in potency, but at the same time, they may be prone to hydrolysis in vivo due to the presence of plasma amidases, leading to rapid clearance. Table 2 shows analogs of compound **2**, including **8** and **9**, where we successively methylated the amide and noted that these compounds suffered a potency loss for the target enzyme. In compound **10**, we reversed the amide linking to the trifluoromethyl phenyl group. This change led to ~2-fold potency improvement for CSF1R and a 10-fold improvement in c-Kit selectivity compared to compound **2**. Next, we consecutively converted each amide to the reduced aminomethyl analog (compounds **11** and **12**). Compound **11** maintained moderate CSF1R potency and selectivity over c-Kit, but compound **12** lost CSF1R inhibition potency, while improving c-Kit potency.

As thiophenes are a known structural alert[14] that are susceptible to reactive metabolite formation[15–18], and have been linked to drug-induced-liver-injury and idiosyncratic toxicities, we embarked on a more comprehensive exploration to replace the thiophene moiety in compound **10**. A variety of heteroaromatic groups were substituted; Table 3 shows chosen compounds with improvements in selectivity over c-Kit and cell potency. Replacing the 2-thiophene with a pyrazole (**14**) and a methyl pyrazole (**13**) resulted in potency and c-Kit selectivity gains and more importantly, BMM cell viability improved to ~81% inhibition when the

Table 1
Initial SAR of bis-amide series.[a]

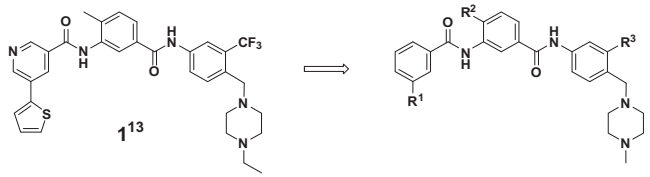

#	R^1	R^2	R^3	CSF1R IC_{50} (μM)	c-Kit IC_{50} (μM)	BMM viability[b]	RAW 264.7 viability[b]
2		Me	CF_3	0.08	0.44	22	7
3		Me	H	>10	>10	11	8
4		Me	Cl	0.23	2.7	20	4
5		Cl	CF_3	0.04	0.19	−7	8
6		Me	CF_3	0.02	0.21	61	6
7		Me	CF_3	0.01	0.31	64	9

[a] Experimental details are in the Supplemental information.
[b] % inhibition @ 1 μM.

Table 2
Linker modifications.[a]

#	Structure	CSF1R IC_{50} (μM)	c-Kit IC_{50} (μM)	Fold selectivity over c-Kit
2	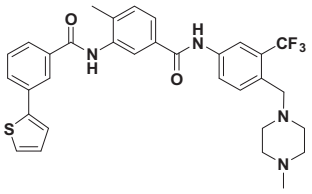	0.08	0.44	5.5
8	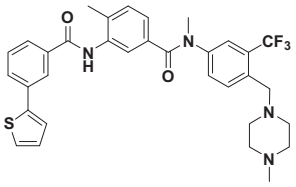	0.63	5.9	9
9	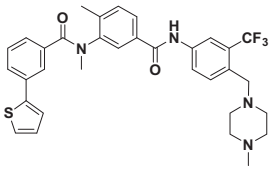	1.8	>10	>6
10	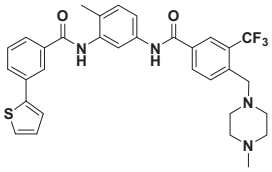	0.03	1.68	56
11	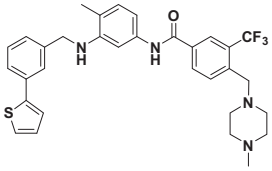	0.35	>10	>29
12	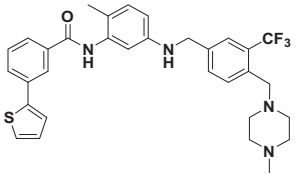	11.7	0.27	<1

[a] Experimental details are in the Supplemental information.

compounds were tested at 1 μM. While the tetrazole analog (**15**) had good biochemical potency and selectivity over c-Kit, the lack of cell viability could be explained by poor cell permeability due to the negatively charged nature of this compound at physiological pH. The 6-membered heteroaryl compounds (**16**, **17**, **18**, **19**) all had potent inhibition of CSF1R. The 2-pyridyl substituted analog (compound **17**) had the best c-Kit selectivity of the series, albeit with a weaker potency in the cell viability (31% inhibition at 1 μM).

In order to assess the potential for oral delivery of these CSF1R inhibitors, we profiled compound **13** with in vitro ADME assays as well as in vivo in a mouse PK study (Table 4). Stability was assessed in NADPH-supplemented mouse and human liver microsomes (MLM, HLM), where modest turnover (47% of parent remaining) was observed in human incubates but high turnover was seen in mouse (7% remaining). As bis-amides might be substrates for plasma amidase activity, we incubated **13** in mouse and human plasma. Compound **13** was stable in human plasma (95% remaining) following a 4 h incubation, however, some degradation was observed in mouse plasma (67% remaining). Kinetic solubility measured in isotonic phosphate buffer was low (5 μM) and suggested that formulating with co-solvents may be necessary for preclinical oral PK studies. Although stability was low in MLM and plasma, we dosed **13** to mice to investigate the PK and demonstrate concordance with the in vitro data. High systemic clearance following intravenous administration was observed, which approximated three times that of liver blood flow in mice (~4.4 L/h/kg)[19], suggesting extrahepatic metabolism, most likely due to plasma instability by hydrolysis. The high systemic clearance may have contributed to high first-pass metabolism when **13** was dosed orally and resulted in low oral bioavailability (12%). Permeability and efflux were not tested for **13**, but would be expected to contribute to the low oral bioavailability as its physicochemical properties violate Lipinski rules (MW > 500 amu and cLogP > 5). Additionally, the positive charge at physiological pH due to the *N*-methyl-piperazine moiety would increase the potential for P-gp efflux.

Considering the poor stability of **13** in mouse liver microsomes, we explored the biotransformation products in NADPH-supplemented MLMs to identify metabolic soft-spots. Metabolite identification (Met-ID) analysis revealed that demethylation at the methyl piperazine of **13** was the major metabolite, with minor hydroxylation sites also noted. The major biotransformation product was putatively suggested to be a simple *N*-demethylation of the piperazine moiety. This was confirmed by preparing an authentic

Table 3
Analogs of compound **10**. SAR of reverse amide series.[a]

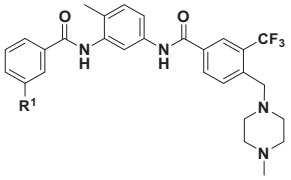

#	R^1	CSF1R IC_{50} (μM)	c-Kit IC_{50} (μM)	Fold selectivity over c-Kit	BMM viability[b,c]
13		0.001	0.74	740	81
14		<0.0005	0.02	>40	80
15		0.02	7.5	375	2.4
16		0.004	0.90	225	84
17		0.012	15	1250	31
18		0.01	0.39	39	72
19		0.009	5.97	663	76

[a] Experimental details are in the Supplemental information.
[b] All compounds had no effect on RAW 264.7 cell viability.
[c] % inhibition @ 1 μM.

Table 4
In vitro and in vivo ADME for compound **13**.[a]

In vitro ADME		
Kinetic solubility (μM)	HLM/MLM (%R)	H/M Plasma (%R)
4.7	46/7	95/67
In vivo mouse PK		
Route	IV	PO
Dose level	2 mg/kg	10 mg/kg
C_{max} (μM)	0.85	0.16
T_{max} (h)	NA	0.25
AUC_{last} (μM·h)	0.27	0.16
$Terminal_{t1/2}$ (h)	0.23	1.32
CL (L/h/kg)	12.6	NA
V_{ss} (L/kg)	4.23	NA
Bioavailability (%)	NA	11.7

H: human, M: mouse, HLM: human liver microsomes, MLM: mouse liver microsomes, %R: percent of parent remaining in incubation relative to time zero control. C_{max}: max plasma concentrations, T_{max}: time of C_{max}, AUC_{last}: area-under-curve from time 0 to last quantifiable concentration, CL; systemic clearance, V_{ss}; volume of distribution at steady-state. Bioavailability: dose normalized ratio of the oral AUC to the IV AUC.
[a] Experimental details are in the Supplemental information.

sample (**20**), which showed the same retention time and product ion spectra as the *N*-demethyl metabolite. Interestingly, when tested in our assay panel, the metabolite (**20**) maintained inhibitory activity against CSF1R and improved c-Kit selectivity (Fig. 2). As expected, based on Met-ID results, the liver microsome stability improved as well. However, the loss in cell-based activity prompted us to question the necessity of the piperazine group.

There are a number of publicly available crystal structures of CSF1R in both DFG-in and DFG-out conformations. Given that it

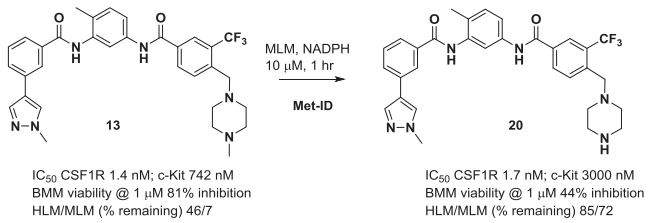

Fig. 2. Results of Met-ID of compound **13**.

was unclear which conformation of CSF1R this series of compounds would bind to, we initially docked **13** into both 3LCD (DFG-in)[20] and 4R7I (DFG-out bound with Imatinib)[7] using Glide.[21] The 3D coordinates of all ligands were generated with LigPrep[22] while the structure was prepared with the Protein Preparation Wizard in Maestro[23] using the default options. It was very clear that **13** appeared to fit much better in the DFG-out conformation of CSF1R. Poses of **13** docked to 3LCD appeared to be strained or could not make interactions with the hinge. However, when docked to 4R7I, **13** bound in a manner very similar to Imatinib. The piperazine in **13** makes key interactions with the protein through Asp796 and His776 while the amide can make hydrogen-bonds with Asp796 and Glu633. The central phenyl ring can make a pi/cation interaction with Lys616. Interestingly, in this pose, the compound does not appear to make a formal hydrogen-bond to the hinge region as is typical in many other kinase inhibitors.

When we removed the piperazine group, compound **21** suffered a 265× loss of potency, which was understandable based on our docking studies (Fig. 3). We reasoned that we needed to include

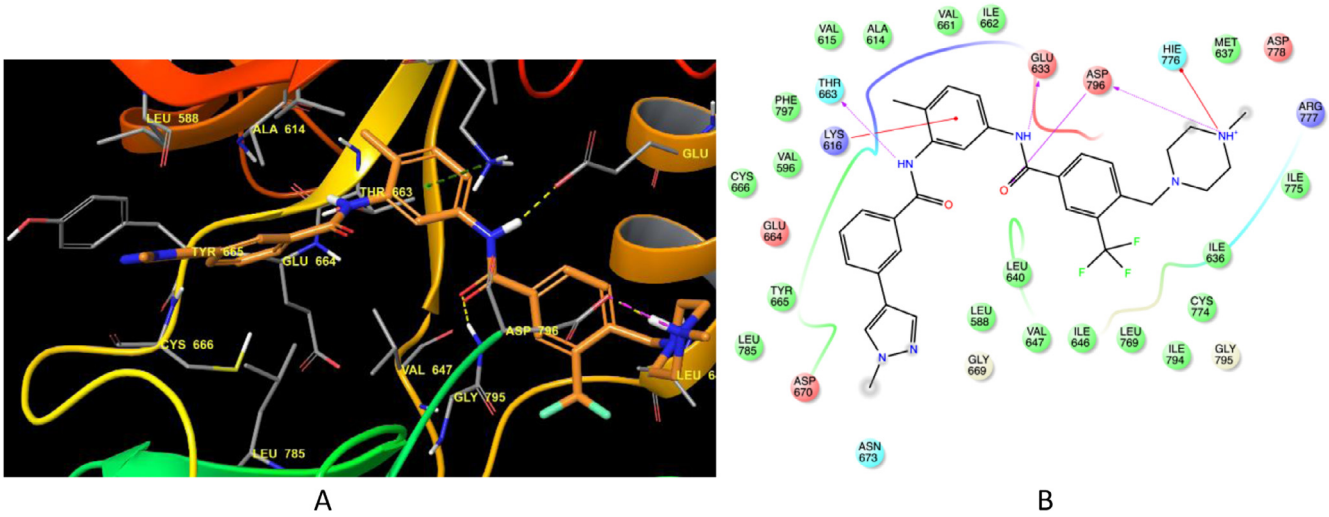

Fig. 3. A) Binding pose and B) Ligand interaction diagram of **13** docked into CSF1R (using 4R7I), highlighting key interactions that the piperazine makes with the protein. Residues and interactions are colored according to the following scheme: Hydrophobic (green), polar (cyan), negatively charged (red), positive charges (purple), glycine (beige), purple arrow (hydrogen-bond), red line (pi-cation). Grey spheres indicate an atom as being solvent exposed.

new functional groups that would interact with the binding pocket of the protein, to regain the lost potency. For this we have docked compound **21**, followed by the design of compounds **22** and **23** which showed us that the introduction of nitrogen atom meta to methylpyrrazole ring picked up the hinge Cys666 interaction (Fig. 4). The core of the molecule is still able to maintain the key hydrogen-bonds with Glu633 and Asp796, as well as the pi-cation interaction with Lys616. Similar docking results were obtained for compound **24** (Figure 5). However, removing the methyl piperazine moiety and introducing an amino-pyrimidine allows the inhibitor to make two new hydrogen bonds to the backbone of Cys666, one between the pyrimidine nitrogen and the backbone N–H, a second between the amino NH_2 and backbone carbonyl of Cys666.

This hypothesis was indeed supported by testing these compounds in the biochemical assay which showed potent CSF1R activity in comparison with compound **21** (Table 5).

BLZ945 is a known ATP competitive CSF1R inhibitor.[24] Most known kinase inhibitors are Type I inhibitors, ATP-competitive compounds such as staurosporine, erlotinib (Tarceva®) and dasatinib (Sprycel®), that bind to the ATP binding site and hydrogen bond with the hinge region of the kinase. Type II inhibitors are compounds which bind partially in the ATP binding site and extend past the gatekeeper and into an adjacent allosteric site that is

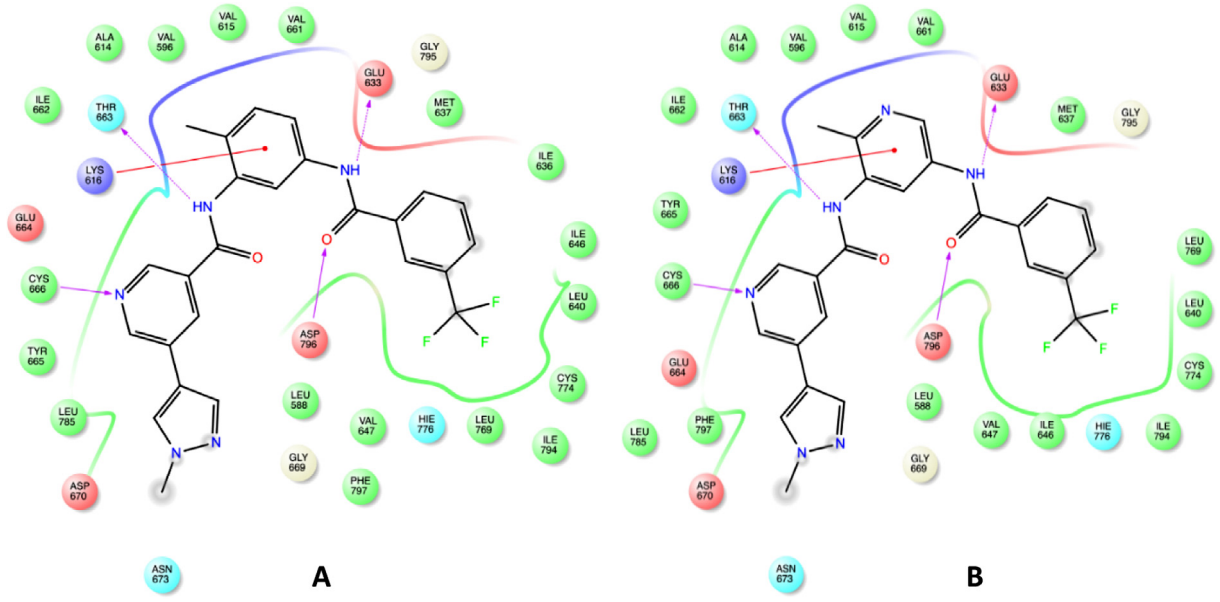

Fig. 4. A) Ligand interaction diagram of **22** and B) **23** docked into CSF1R. In both docked poses, the conserved hydrogen-bond interactions between the inhibitor and Glu633 and Asp796, as well as the pi-cation interaction with Lys616, are well maintained. In addition, there is a possible hydrogen-bond interaction between the side chain of Thr663 and the amide NH. Replacing the phenyl ring, adjacent to the methyl piperazine moiety, by a pyridine allows the inhibitor to make a hydrogen-bond with the backbone carbonyl of Cys666, located in the hinge region, improving potency. Residues and interactions are colored according to the following scheme: Hydrophobic (green), polar (cyan), negatively charged (red), positive charges (purple), glycine (beige), purple arrow (hydrogen-bond), red line (pi-cation). Grey spheres indicate an atom as being solvent exposed.

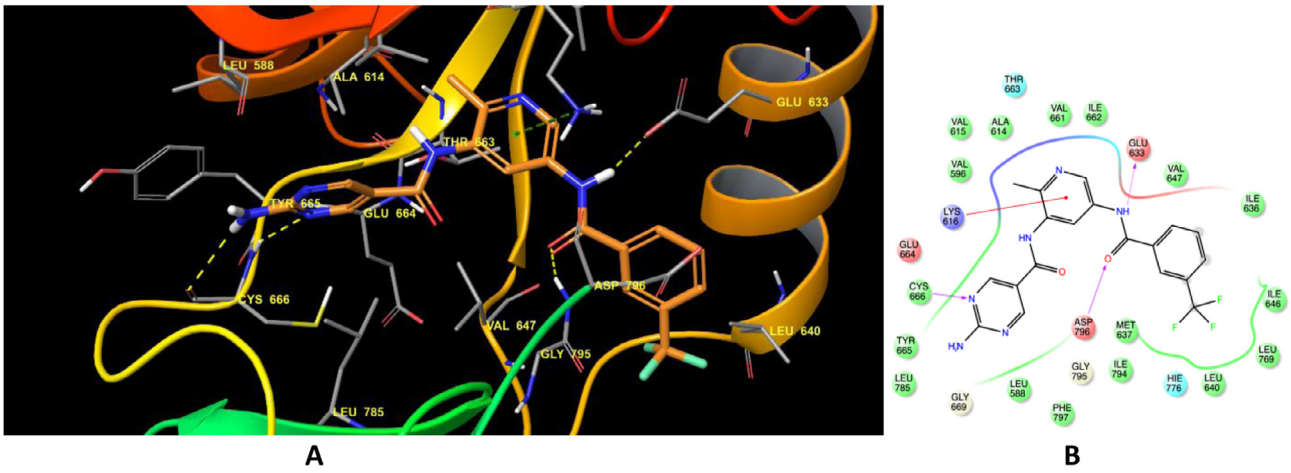

Fig. 5. A) Binding pose and B) Ligand interaction diagram of **24** docked into CSF1R (using 4R7I). Residues and interactions are colored according to the following scheme: Hydrophobic (green), polar (cyan), negatively charged (red), positively charged (purple), glycine (beige), purple arrow (hydrogen-bond), red line (pi-cation). Grey spheres indicate an atom as being solvent exposed.

Table 5
SAR leading to removal of the *N*-methyl piperazine.[a]

#	Structure	CSF1R IC_{50} (μM)	c-Kit IC_{50} (μM)	Fold selectivity over c-Kit	BMM viability[b,c]	HLM/MLM (% rem)
13	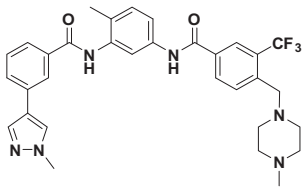	0.001	0.74	740	81	46/7
21	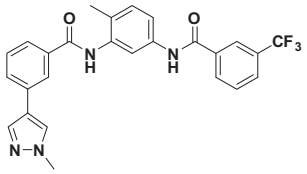	0.37	0.13	0.35	ND	68/74
22	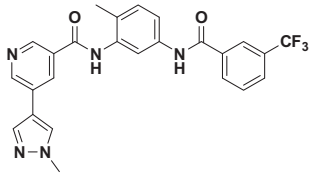	0.0005	0.06	120	96	37/63
23	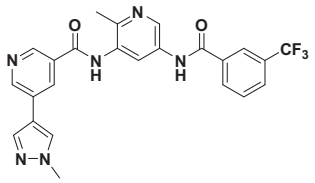	0.0009	0.18	200	87	60/57
24	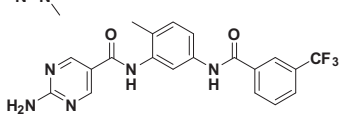	0.032	0.82	25	86	91/65

[a] Experimental details are in the Supplemental information.
[b] All compounds had no effect on RAW 264.7 cell viability.
[c] % inhibition @ 1 μM.

present only in the inactive kinase conformation. Imatinib is a well-known Type II inhibitor. As our docking studies indicated that **13** bound in a manner similar to imatinib, we explored the mechanism of inhibition of a few selected molecules via a biochemical assay. Compounds **13** and **22** which were seen to pick up key interactions with the CSF1R protein, based on docking studies, were chosen and compared with **BLZ945** binding in the presence of variable concentrations of ATP. While **BLZ945** showed a ~30-fold increase in IC_{50} at 500 μM ATP (40X Km ATP for CSF1R enzyme), **13** showed minimal change in IC_{50} at similar ATP concentration

Table 6
Caco2 permeability of Compounds **22**, **23** and **24**.[a]

#	A2B		B2A		Efflux Ratio (A2B/B2A)
	Mean P_{app} (10^{-6} cms^{-1})	SD	Mean P_{app} (10^{-6} cms^{-1})	SD	
22	12.5	0.81	32.5	0.47	2.6
23	0.5	0.04	36.3	3.34	81.5
24	0.1	0.00	5.3	0.38	40.4

A2B: apical to basolateral (absorption) direction, B2A: basolateral to apical (secretory) direction, P_{app}, apparent permeability; Efflux ratio; B2A/A2B.
[a] Experimental details are in the Supplemental information.

Table 7
Mouse PK of Compound **22**.[a]

Route	IV	PO
Dose level	2 mg/kg	10 mg/kg
C_{max} (μM)	3.55	4.60
T_{max} (h)	NA	0. 50
AUC_{last} (μM·h)	2.24	6.94
Terminal$_{t1/2}$ (h)	0.87	1.80
CL (L/h/kg)	1.86	NA
V_{ss} (L/kg)	1.10	NA
Bioavailability (%)	NA	64.0

C_{max}: max plasma concentrations, T_{max}: time of C_{max}, AUC_{last}: area-under-curve from time 0 to last quantifiable concentration, CL: systemic clearance, V_{ss}: volume of distribution at steady-state. Bioavailability: dose normalized ratio of the oral AUC to the IV AUC.
[a] Experimental details are in the Supplemental information.

and **22** showed only marginal (~6-fold) increase in IC_{50} at 500 μM ATP (Supplemental information). This indicated that unlike **BLZ945** which behaves in a purely competitive fashion with respect to ATP, both **13** and **22** behave differently and were more like Type II inhibitors that are mildly ATP competitive or are non-competitive with ATP. This biochemical study validates the choice of the DFG-out configuration for the modeling studies and supports the predicted binding mode based on docking studies.

Compounds **22**, **23** and **24** were tested for their in vitro stability in NADPH-supplemented human and mouse liver microsomes. They were found to be more stable in MLM with moderate turnover (range 57–65% remaining), relative to compound **13**. Additionally, we studied these new lead compounds in a Caco2 permeability assay and found that there were a range of permeabilities and efflux values for these analogs (Table 6). Both **23** (Papp = 0.5 × 10^{-6} cm/s) and **24** (Papp = 0.1 × 10^{-6} cm/s) demonstrated low absorptive permeability (apical to basolateral direction), while **22** demonstrated high absorptive permeability (Papp = 12.5 × 10^{-6} cm/s). All three compounds, however, were effluxed by Caco2 membrane transporters with secretory (basolateral to apical) to absorptive (apical to basolateral) permeability ratios values of 2.6 (**22**), 40 (**23**) and 82 (**24**) (Table 6). Based on its higher absorptive permeability and lower efflux, the oral absorption of **22** would not be expected to be impacted by slow absorption or efflux back into the lumen of the gut.

Compound **22** was further evaluated in a mouse PK study, where systemic clearance was substantially reduced (50% of mouse hepatic blood flow) compared to **13** and the oral bioavailability was increased (64%) as shown in Table 7. These data are consistent with improved metabolic stability, permeability and solubility (38 μM) compared to compound **13**.

The synthesis of the compounds **2**–**5** in Table 1 followed the sequence of steps described in Scheme 1. Synthesis started with the coupling of acid **I** with amines **II** and **VIII** to provide the ester compounds **III** and **IX**. These esters were then hydrolyzed using NaOH to provide the corresponding acids **IV**, **X**, which were then subjected to amide coupling with various 3-substituted 4-((4-methylpiperazin-1-yl) methyl) anilines **V**, **VI** and **VII** to give the bisamides **2**–**5**.

The synthesis of the compounds **10**, **13**–**14**, **16**, **18**–**19** in Table 3 followed the sequence of steps described in Scheme 2. The commercially available amine **XXI** was coupled with acid **XXII** to provide the bromo bisamide **XXIII** which were then coupled with various heterocyclic boronates resulting in compounds **10**, **13**–**14**, **16**, **18**–**19**.

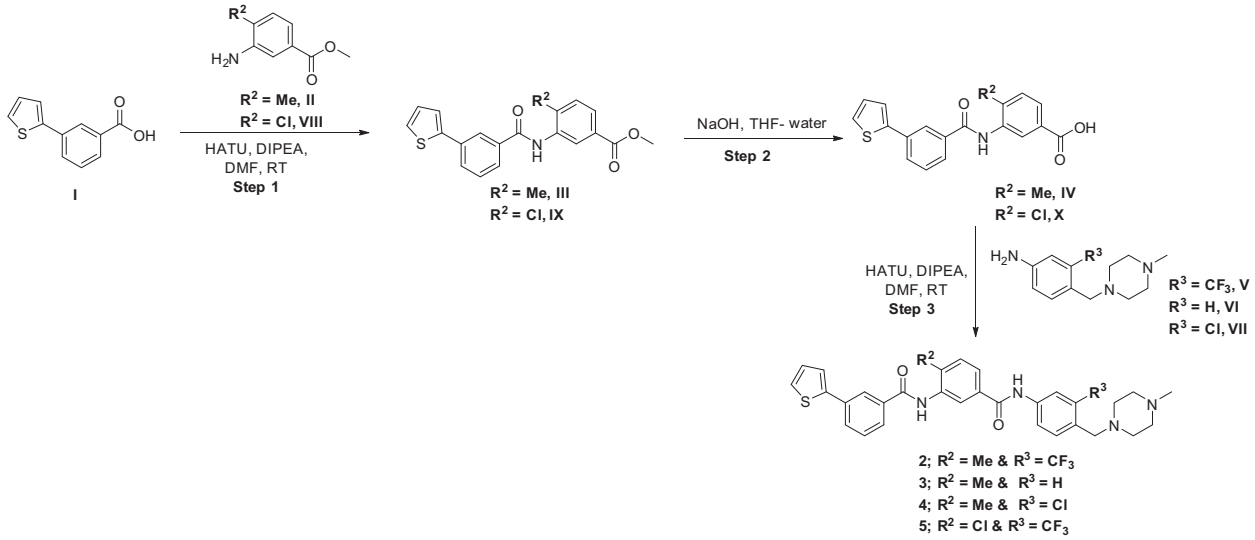

Scheme 1. Synthesis of compounds **2**–**5**.

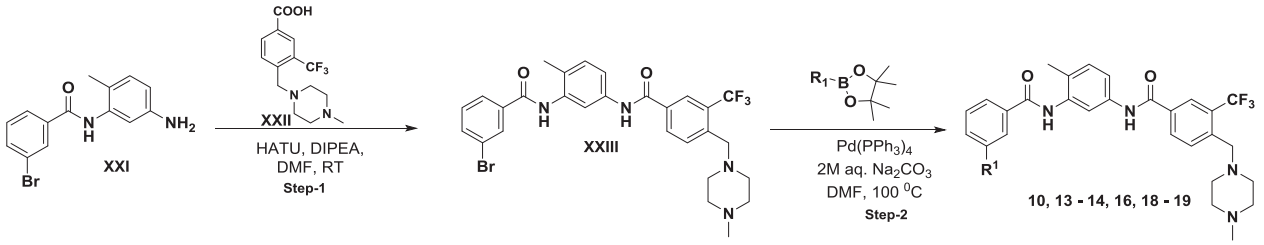

Scheme 2. Synthesis of compounds **10**, **13**–**14**, **16**, **18**–**19**.

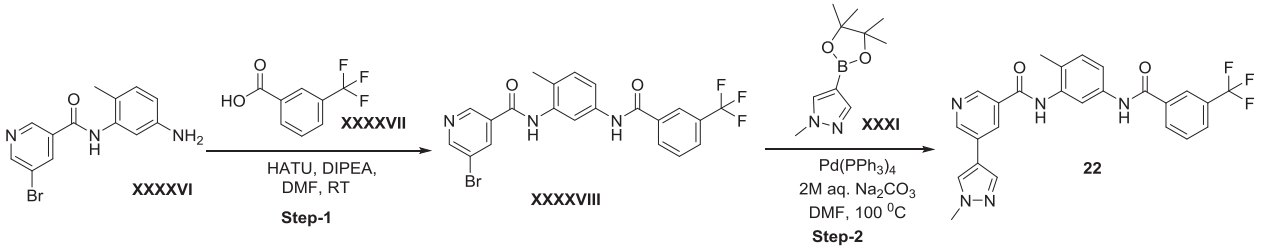

Scheme 3. Synthesis of compound **22**.

Compound **22** was synthesized as described in Scheme 3. The commercially available amine **XXXXVI** was coupled with 3-(trifluoromethyl) benzoic acid to provide the bromo bisamide **XXXXVIII** which underwent a Suzuki coupling with methypyrazole-4-boronic acid resulting in compound **22**.

Compounds **6**–**9**, **11**–**12**, **15**, **17**, **20**–**21**, **23**–**24** were synthesized by alternative routes (see Supporting information).

In this manuscript, we have described the synthesis and optimization of CSF1R inhibitors. Initial leads contained an *N*-methyl piperazine group that was required for activity, but was metabolically labile, contributing to a poor mouse pharmacokinetic profile. Biochemical and docking analysis allowed us to remove the *N*-methyl piperazine group, while introducing other hydrogen-bonding interactions with the binding pocket of CSF1R. Removal of this group also afforded better physicochemical properties by reducing the molecular weight, charge and number of hydrogen bonding acceptors/donors. Through this approach, we could design and synthesize new compounds with more potent inhibition of CSF1R and improved cellular efficacy. By virtue of better physicochemical properties, our lead compound **22**, also showed good intestinal permeability in a Caco2 assay and favorable pharmacokinetics when dosed orally to mice. This compound appears suitable for in vivo pharmacology testing in the appropriate preclinical tumor model to demonstrate proof of concept. Future work could be focused on optimizing this lead for cancer applications.

Funding: This research did not receive any specific grant from funding agencies in the public, commercial or not-for-profit sectors. It was funded by Medivation, now Pfizer.

Acknowledgements

The authors thank Stacy Kanno, Teresa Kameda, Ramona Almirez, Katherine Stack, Walter Yu and Sunny Chen for in-life and bioanalysis work and the Analytical and Purification group at Integral Bioscience for purification of compounds and for acquiring relevant analytical data.

A. Supplementary data

Supplementary data associated with this article can be found, in the online version, at http://dx.doi.org/10.1016/j.bmcl.2017.03.064.

References

1. Hamilton JA. *Nat Rev Immunol.*. 2008;8:533–544.
2. Ruffell B, Coussens LM. *Cancer Cell.*. 2015;27:462–472.
3. Noy R, Pollard JW. *Immunity.*. 2014;41:49–61.
4. Ries CH, Hoves S, Cannarile MA, Ruttinger D. *Curr Opin Pharmacol.*. 2015;23:45–51.
5. Pyonteck SM, Akkari L, Schuhmacher AJ, et al. *Nat Med.*. 2013;19:1264–1272.
6. Zhu Y, Knolhoff BL, Meyer MA, et al. *Cancer Res.*. 2014;74:5057–5069.
7. Tap WD, Wainberg ZA, Anthony SP, et al. *N Engl J Med.*. 2015;373:428–437.
8. <https://www.clinicaltrials.gov/ct2/results?term=PLX7486&Search=Search>.
9. Company website: <http://www.arraybiopharma.com/product-pipeline/other-compounds/arry-382/>.
10. von Tresckow B, Morschhauser F, Ribrag V, et al. *Clin Cancer Res.*. 2015;21:1843–1850.
11. Lennartsson J, Ronnstrand L. *Physiol Rev*. 2012;92:1619–1649.
12. Hume DA, MacDonald KP. *Blood.*. 2012;119:1810–1820.
13. Choi Y, Syeda F, Walker JR, et al. *Bioorg Med Chem Lett.*. 2009;19:4467–4470.
14. Kalgutkar AS, Gardner I, Obach RS, et al. *Curr Drug Metab.*. 2005;6:161–225.
15. Wu G, Vashishtha SC, Erve JC. *Chem Res Toxicol.*. 2010;23:1393–1404.
16. Dansette PM, Libraire J, Bertho G, Mansuy D. *Chem Res Toxicol.*. 2009;22:369–373.
17. Ono K, Kurohara K, Yoshihara M, Shimamoto Y, Yamaguchi M. *Am J Hematol.*. 1991;37:239–242.
18. Koenigs LL, Peter RM, Hunter AP, et al. *Biochemistry.*. 1999;38:2312–2319.
19. Davies B, Morris T. *Pharm Res.*. 1993;10:1093–1095.
20. Meyers MJ, Pelc M, Kamtekar S, et al. *Bioorg Med Chem Lett.*. 2010;20:1543–1547.
21. Glide v7.2; Schrödinger Inc: Portland, OR.
22. LigPrep v3.9; Schrödinger Inc: Portland, OR.
23. Glide v10.7; Schrödinger Inc: Portland, OR.
24. Daniel D, Joyce J, Sutton J. WO2012/151541 A1.